P4

Publication 4

E. Ikonen, P. Manninen, and P. Kärhä, "Modeling distance dependence of LED illuminance," *Light & Engineering* Vol. **15,** No. 4, 57–61 (2007).

Light & Engineering
Vol. 15, No. 4, pp. 57—61, 2007

Svetotekhnika
No. 6, 2007, pp. 46–49

MODELING DISTANCE DEPENDENCE OF LED ILLUMINANCE*

Erkki Ikonen[1,2], Pasi Manninen[1], and Petri Kärhä[1],

[1] *Metrology Research Institute, Helsinki University of Technology (TKK), PO Box 3000, FI-02015 TKK, Finland*
[2] *Centre for Metrology and Accreditation (MIKES), PO Box 9, FI-02151 Espoo, Finland*
E-mail: erkki.ikonen@tkk.fi

A method for determining photometric properties of an LED in terms of its axial luminous intensity, angular intensity pattern, and radius and location of the effective LED source is presented. The applicability of the method was tested for seventeen LED types with different packages, angular intensity distributions, and power levels. When applying the developed method to the measurement data, instead of the inverse-square law of a point source, a significant reduction in the distance dependence of apparent LED luminous intensity was achieved.

1. INTRODUCTION

The definition of measurement conditions for the optical properties of LED light sources continues to be one of the focal points of the Technical Committees of the CIE. Methods have been presented for measuring the position of the LED source to determine a reliable luminous intensity value of the LED [1,2]. However, these analyses necessitate that the exact radius of the emitting area of the LED is known. Another possibility is to treat the LED as just a simple point source. This article reviews some of the limitations of the conventional point-source analysis and presents an improved method [3] which can be used to determine the illuminance at variable distances from an LED. The method is closely related to the earlier analyses of the distance dependence of signal with photometers [4] and spectroradiometers [5, 6, 7] equipped with diffusers.

To be able to predict the LED illuminance at any distance, the method utilizes a two-aperture model with an extended source and detector [3]. It describes energy transfer between parallel circular plates, centered on the optical axis of the measurement system. The method can also account for a highly non-Lambertian, directional angular intensity distribution of the LED source. Details of the derivation of the model equations are presented for the first time in this article. The behavior of the LED illuminance is described by its axial luminous intensity, angular intensity pattern, and radius and location of the effective LED source. The parameters of the model can be determined from illuminance measurements at a few distances from the LED.

When applying the developed method to the measurement data, instead of a point-source model, the distance dependence of apparent LED luminous intensity of up to 50 % reduced to statistical variation of less than 1 % for all the seventeen tested LED types [3]. In this article it is further shown that in many cases a simplified analysis method can be used, which leads to significant reduction of the needed experimental effort and still yields results of sufficient reliability. The analysis of the data leads to the satisfactory conclusion that an unambiguous luminous intensity value can be used for calculating the LED illuminance over a broad distance range.

2. LIMITATIONS OF POINT-SOURCE ANALYSIS

The luminous intensities I_v of seventeen different types of LEDs were determined at various distances

* On basis of presentation on 26th CIE Session, July 2007, Beijing.

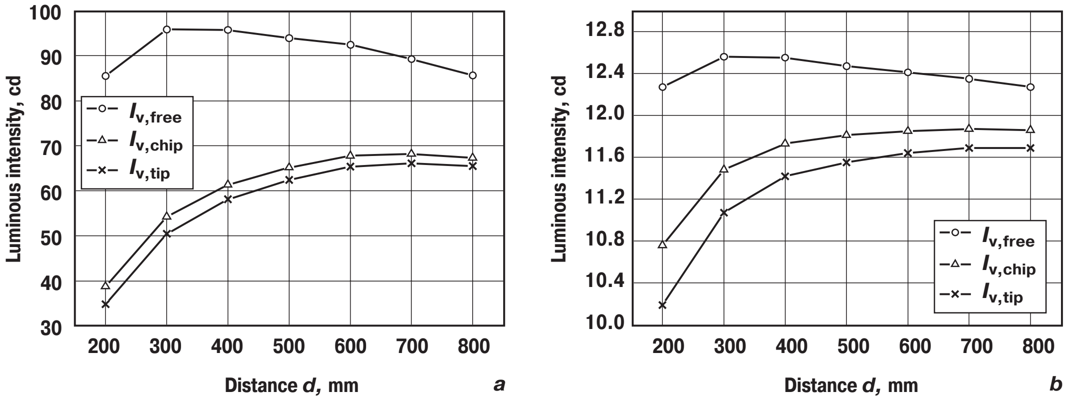

Fig. 1. Luminous intensities $I_{v,tip}$, $I_{v,chip}$ and $I_{v,free}$ of LED #14 (*a*) and LED #12 (*b*) as a function of distance (see text for details)

d. The measured illuminance values $E_v(d)$ were first assumed to obey the inverse-square law for a point source,

$$E_v(d) = \frac{I_{v,tip/chip}}{(d+\Delta d)^2} \tag{1}$$

relative to two reference planes for the LED, i.e., the front tip of the LED (distance offset $\Delta d = 0$) and the site of the LED chip ($\Delta d > 0$). A clear distance dependence of the obtained luminous intensity values occurred in the analysis with respect to both reference planes. Then the reference plane position Δd was allowed to vary freely, but still more than half of the tested LED types showed distance dependence of the corresponding luminous intensity $I_{v,free}$. Examples from measurements with two of the LEDs are shown in Fig. 1. These were unsatisfactory results due to the need of large amount of measurements for the full LED illuminance characterization.

3. DERIVATION OF MODEL EQUATIONS

Fig. 2 describes a circular source (radius r_0) and a circular detector (radius r'_0) at a distance D from each other. The planes of the source and detector are parallel and their centers are located on the z axis (optical axis) of a cylindrical coordinate system. The radiant flux emitted by a small surface element dA at (r, φ, 0) to the detector surface element dA' at (r', φ', D) is $d\Phi_e = L_e(r, \varphi; \theta) dA_\perp d\Omega$, where $L_e(r, \varphi; \theta)$ is the radiance at position (r, φ, 0) in the direction θ relative to the normal of the surface, $dA_\perp = dA\cos\theta$ is the projected area of dA in the direction θ, and $d\Omega = dA'\cos\theta / R^2$ is the solid angle defined by point (r, φ, 0) and the surface element dA' at the distance R. A homogeneous source with angular dependence $L_e(r, \varphi; \theta) = L_0 \cos^{n-1}\theta$ of the radiance is assumed, where L_0 does not depend on r or φ and the parameter n indicates the degree of the directivity of the source. For a Lambertian source, the directivity parameter has a value $n = 1$. With these definitions the spectral radiant intensity of the source becomes $I_e(\theta) = I_0 \cos^n\theta$, where $I_0 = \pi r_0^2 L_0$ is the axial radiant intensity of the source.

The total radiant flux emitted by the source to the detector is obtained by integrating $d\Phi_e$ over all surface elements $dA = r d\varphi dr$ and $dA' = r' d\varphi' dr'$. The distance dependence of spectral irradiance at the detector is thus

$$E_e(D) = \frac{\iint\limits_{AA'} d\Phi_e}{\pi r_0'^2} = \frac{I_0}{\pi^2 r_0^2 r_0'^2} \iint\limits_{AA'} \frac{\cos^{n+1}\theta \, dA dA'}{R^2}. \tag{2}$$

Since $\cos\theta = D/R$ and $R^2 = D^2 + r^2 + r'^2 - 2rr'\cos(\varphi - \varphi')$, Eq. (2) can be written as

$$E_e(D) = \frac{I_0 D^{n+1}}{\pi^2 r_0^2 r_0'^2} \times$$

$$\times \int_0^{2\pi}\int_0^{2\pi}\int_0^{r_0}\int_0^{r'_0} \frac{rr' d\varphi d\varphi' dr dr'}{[D^2 + r^2 + r'^2 - 2rr'\cos(\varphi - \varphi')]^{(n+3)/2}}. \tag{3}$$

The integration of Eq. (3) can be carried out analytically when $n = 1$ [8]. Next we approximate the square root of the denominator of Eq. (3) using the fact that D is much larger than either r or r',

$$\left\{ D^2 \left[1 + \frac{r^2 + r'^2 - 2rr'\cos(\varphi - \varphi')}{D^2} \right] \right\}^{(n+3)/4} \approx$$

$$\approx D^{(n+3)/2}\left[1+\frac{n+3}{4}\frac{r^2+r'^2-2rr'\cos(\varphi-\varphi')}{D^2}\right]=$$

$$=D^{(n-1)/2}[D^2+\rho^2+\rho'^2-2\rho\rho'\cos(\varphi-\varphi')], \quad (4)$$

where $\rho = r(n+3)^{1/2}/2$ and $\rho' = r'(n+3)^{1/2}/2$. Terms of order $(r/D)^4$, $(r'/D)^4$, $(rr'/D^2)^2$, r^3r'/D^4, rr'^3/D^4, and higher are neglected in Eq. (4).

When Eq. (4) is substituted into Eq. (3), a result is obtained,

$$E_e(D)=\frac{I_0D^2}{\pi^2 r_S^2 r_D^2}\times$$

$$\times\int_0^{2\pi}\int_0^{2\pi}\int_0^{r_S}\int_0^{r_D}\frac{\rho\rho' d\varphi d\varphi' d\rho d\rho'}{[D^2+\rho^2+\rho'^2-2\rho\rho'\cos(\varphi-\varphi')]^2}, \quad (5)$$

which is of the same form as Eq. (3) with $n = 1$ taking into account that r_0 and r_0' are replaced by the effective source and detector radii

$$r_S=\frac{r_0}{2}\sqrt{n+3} \text{ and } r_D=\frac{r_0'}{2}\sqrt{n+3}, \quad (6)$$

respectively [3,6]. As mentioned above, the equation for spectral irradiance can then be integrated exactly over the source and detector surfaces [8]. After $V(\lambda)$-weighted integration of the spectral irradiance, the distance dependence of source illuminance is finally obtained,

$$E_v(d)=\frac{I_{v,\text{eff}}}{(d+\Delta d)^2+r_S^2+r_D^2}g(d), \quad (7)$$

where $I_{v,\text{eff}}$ is the effective luminous intensity of the source on the measurement axis, $D = d + \Delta d$ is written as a sum of the nominal distance d and distance offset Δd, and

$$g(d)=\frac{2}{1+\sqrt{1-4r_S^2r_D^2/[(d+\Delta d)^2+r_S^2+r_D^2]^2}} \quad (8)$$

is a geometrical factor, specific to the circular source and detector.

Eqs. (6–8) are applied to rigorous analysis of LED illuminance data $E_v(d)$ at different distances d from the front tip of the LED. Angular LED intensity distribution measurement first determines the directivity parameter n. Then Eq. (7) is fitted to the distance dependence data using $I_{v,\text{eff}}$, Δd, and r_0 as the fitted parameters, while parameters n and r_0' are fixed to the known values. Factor $g(d)$ is usually close to 1, but it is retained in the rigorous analysis in its complete form, since for highly directional LEDs,

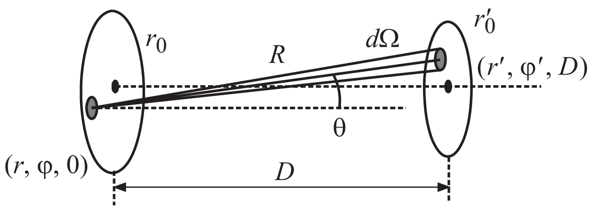

Fig. 2. Geometrical parameters for derivation of the model equations

equations (6) amplify the effect of the source and detector radii in such a way that the obtained luminous intensity may be affected by a few percents if approximation $g(d) \approx 1$ is used.

After deriving the complete equations for the distance dependence of LED illuminance, one may ask if the parameters n and $g(d)$ are always necessary for the analysis. Clearly, if n is close to 1 and d is much larger than Δd, r_0, and r_0', a good approximation of Eq. (7) is given by

$$E_v(d)=\frac{I_{v,\text{eff}}}{(d+\Delta d)^2+r_0^2+r_0'^2}, \quad (9)$$

which is obtained by fixing $n = g(d) = 1$ in Eqs. (6) and (7). The conditions for the validity of Eq. (9) will be addressed in Sec. 5 using synthesized LED illuminance data based on the rigorous model Eqs. (6–8).

4. EXPERIMENTAL

A commercial LED photometer manufactured by LMT Lichtmesstechnik GmbH was used in the illuminance measurements. The photometer has a circular entrance aperture with a radius of $r_0' = 5.64$ mm. A planar diffuser is used behind the aperture to improve the angular responsivity of the photometer. The distance offset of the photometer reference plane position from the front surface of the diffuser is zero. The photometer was calibrated for the illuminance responsivity against an absolutely characterized reference photometer.

The developed method was tested with seventeen different types of LEDs having a variety of packages, beam geometries, and power levels [3]. The tested LEDs were mounted, one by one, on a specific holder made of PVC (polyvinyl chloride) and aluminum. Constant current of 330 mA was used for the high-power LEDs of 1 W and 20.0 mA for the other LEDs. The illuminance measurements were performed on a 4.5-m optical rail using a magnetic length measuring device with 0.1 mm resolution. Measurements were made at seven distances in various distance ranges between $d = 50$ mm and $d = 3000$ mm depending on the power level of the tested LED.

The photometer was mounted on a rail carrier and the tested LEDs were placed to the other end of the optical rail. The mechanical symmetry axis of the tested LED was aligned perpendicular to the receiving aperture of the photometer and to cross the center point of the photometer aperture by using a two-beam alignment laser and an alignment mirror. To get the correct orientations for the tested LEDs, aluminum bodies with bore diameters of 6 mm and 12 mm were used for the LED alignments. For photometer signal measurement, a digital voltmeter was connected to a measurement computer via the IEEE-488 bus. Dark current was measured before the signal measurements utilizing an electronic shutter also controlled through the serial bus.

5. RESULTS AND ANALYSES

The distance dependence of illuminance was measured for the different LEDs. The method based on Eqs. (6–8) was used in the analysis of the data. Fig. 3 shows examples of the results for the same LEDs as used in the measurements of Fig. 1. Comparing Figs. 1 and 3, it can be seen that in case of LED #14 (#12) the distance dependence of LED illuminance of 50 % (10 %) is reduced to statistical fluctuation with a standard deviation of 0.7 % (0.1 %). The tested LED #14 is 10-mm-type TLOH190P of 4° half-value angle $\Delta\Theta$ (full width at half maximum, FWHM) and LED #12 is of type E1L51-YC1A with $\Delta\Theta = 8°$.

The fitting results of the data of Fig. 3(a) are $I_{v,eff} = 61.2$ cd, $\Delta d = -73$ mm, and $r_0 = 10$ mm. The directivity parameter is $n = 1915$, resulting in $g(d) = 1.15$ at the closest used distance $d = 200$ mm. When the data analysis was repeated with a fixed value $g(d) = 1$, the value of fitted luminous intensity $I_{v,eff}$ increased from 61.2 cd to 64.0 cd and its peak-to-peak variation from 2.0 % to 2.4 %. The fitting results of the data of Fig. 3(b) are $I_{v,eff} = 11.7$ cd, $\Delta d = -5.4$ mm, and $r_0 = 5$ mm. The directivity parameter is $n = 590$, resulting in $g(d) = 1.008$ at $d = 200$ mm.

The data analysis by Eqs. (6–8) gave a value of $r_0 \leq 0.1$ mm for seven LED types. These LEDs had $n \leq 45$ and they can be reasonable well described by a point-source model. For some LEDs, the point source appears to be located at the site of the LED chip. However, for ten LED types it was necessary to allow values of r_0 between 1 and 12 mm in order to obtain a luminous intensity $I_{v,eff}$ which does not depend on the measurement distance. All of these LEDs are not high-n types, since half of them had directivity parameter values less than 30. Figs. 1 and 3 illustrate the significant improvement in the consistency of the luminous intensity values $I_{v,eff}$ as obtained by the analysis method of Sec. 3.

It is of interest to determine such a value of the directivity parameter n, below which the luminous intensity analysis can be made reliably using the simplified Eq. (9). Thus, simulated illuminance values were calculated by Eqs. (6–8) for the distance range 200–800 mm with various values of the directivity parameter n and typical values of the distance offset and source radius. These synthesized data were then analyzed using the simplified Eq. (9) and the fitting results were compared with the original parameter values. Fig. 4 shows examples of the results of these tests, where the relative deviation of the obtained luminous intensity is plotted as a function of the directivity parameter n.

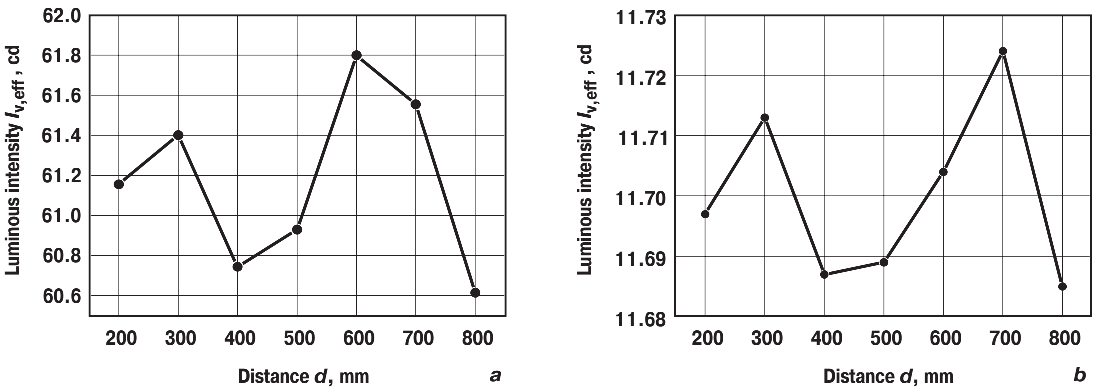

Fig. 3. Luminous intensity $I_{v,eff}$ as a function of distance for LED #14 (*a*) and LED #12 (*b*). The relative peak-to-peak variations of 2 % (*a*) and 0.3 % (*b*) are smaller than those in Fig. 1 by a factor of 5 to 20

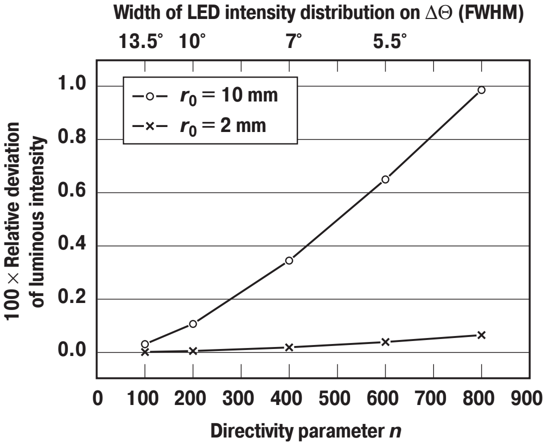

Fig. 4. Relative deviation of the obtained luminous intensity using two different analysis methods. The FWHM width $\Delta\Theta$ of the LED intensity distribution is indicated by the upper scale. The used distance offset was Δd = 10 mm

It is concluded from these analyses that data fitting using Eq. (9) can be made with good accuracy when the width (FWHM) of the LED intensity distribution is larger than 10°. Such a width corresponds to the directivity parameter value n = 200.

6. CONCLUSIONS

Applicability of the developed method has been demonstrated with seventeen different LED types, for which also the luminous intensities according to the point-source approximation were determined. When applying the method to the measurement data, the distance dependence of apparent LED luminous intensity decreased dramatically as compared with the analysis results based on the point-source approximation. Significant simplification of the developed method can be achieved when analyzing LEDs with broad beams. When the half-width angle is larger than 10°, the luminous intensity of the LED can be determined sufficiently accurately without detailed information on the angular intensity distribution.

The developed method gave notably consistent results for the luminous intensities measured at different distances, their standard deviation being less than 0.3 % for most of the tested LEDs. The LED manufacturers could measure and specify luminous intensity values for their LEDs using the methods described in Sec. 3. The photometric behaviour of designed light systems could then be estimated more reliably before constructing prototypes, which might lead to considerable savings in development costs.

REFERENCES

1. Muray K, Proc. Soc. Photo-opt. 954, 1988, pp. 560–567.
2. Muray K, Appl. Opt. 30, 1991, pp. 2178-2186.
3. Manninen P, Hovila J, Kärhä P, and Ikonen E, Meas. Sci. Technol. 18, 2007, pp. 223-229.
4. Hovila J, Mustonen M, Kärhä P, and Ikonen E, Appl. Opt. 44, 2005, pp. 5894-5898.
5. Manninen P, Hovila J, Seppälä L, Kärhä P, Ylianttila L, and Ikonen E, Metrologia 43, S120-S124 (2006).
6. Ikonen E, Manninen P, Hovila J, and Kärhä P, in Proceedings of Metrology Symposium 2006, Queretaro, Mexico, 2006 (CD, 5 p.).
7. Gröbner J and Blumthaler M, Optics Letters 32, 2007, pp. 80-82.
8. Walsh J W T, Photometry (New York: Dover, 1965), pp. 120–73.

Erkki Ikonen
received the M.Sc. and Dr.Sc.(Tech.) degrees in engineering from the Helsinki University of Technology, in 1982 and 1988, respectively. His research for the last 15 years has been directed toward development of laser-based measurements, high-accuracy instruments for interferometry, and improved methods for radiometric and photometric measurements

Petri Kärhä
received his M.Sc. and D.Sc. degrees in electrical engineering from the Helsinki University of Technology in 1993 and 1997 respectively

Pasi Manninen
received his MSc degree in electrical engineering from the Helsinki University of Technology in 2004. He is currently pursuing the doctor of technology degree in TKK